Frame Arrival Timing in LoRaWAN: Capacity Increase With Repeated Transmissions and More Channel Attenuation

Martin Heusse, Christelle Caillouet, Andrzej Duda

Frame Arrival Timing in LoRaWAN: Capacity Increase With Repeated Transmissions and More Channel Attenuation

Martin Heusse
Univ. Grenoble Alpes,
CNRS, Grenoble INP, LIG
Grenoble, France
Martin.Heusse@imag.fr

Christelle Caillouet
Université Côte d'Azur, I3S,
CNRS, Inria,
Sophia Antipolis, France
Christelle.Caillouet@univ-cotedazur.fr

Andrzej Duda
Univ. Grenoble Alpes,
CNRS, Grenoble INP, LIG
Grenoble, France
Andrzej.Duda@imag.fr

***Abstract*—This paper considers a LoRaWAN cell in which devices access the channel using the unslotted ALOHA protocol. We propose a model of this access method that combines the effects of collisions with channel fading, by which reception may get buried in noise. Unlike the existing models of LoRaWAN, our model takes into account the frame arrival timing: it distinguishes, on the one hand, the interference created by earlier transmissions with respect to the frame of interest, and on the other hand, the interference by the frames arriving later on.**

From the results of the model, we draw three observations regarding the improvement of Packet Delivery Ratio (*PDR*). First, it puts back under the spotlight the often overlooked fact that repeating frames is always beneficial when the desired *PDR* is above 60%, even though the extra packet transmissions create more collisions. Second, as soon as the node density becomes notable and collisions have a similar impact on losses as attenuation, adding a smaller spreading factor *SF6* modulation into the cell list of transmission parameters allows increasing the coverage range. Third, the model shows that cell capacity sometimes grows with the distance to the gateway or with decreased node transmission power, a trend seldom observed in wireless networks.

I. Introduction

LoRa is a recent LPWAN (Low Power Wide Area Networks) technology that supports low-power long range communications oriented towards IoT (Internet of Things) applications [1]. It uses a specific radio layer based on the CHIRP Spread Spectrum (CSS) modulation that gives access to a number of data rates which provide various levels of transmission robustness. LoRaWAN [2] specifies a communication protocol over the physical layer and the network architecture. For uplink communications, we focus on Class A (for All devices) in which the devices access the channel exclusively using the unslotted ALOHA protocol [3], [4]: a device wakes up and can send a packet at any instant on a chosen radio channel, provided its duty cycle follows the frequency band regulations (typically 1 % in the 868 MHz band under EU regulations). One or several Gateways (GW) may receive the packet and forward it to Network and Application Servers. After sending a packet, a device opens two short reception windows for downlink communication.

As sending downlink packets to a large number of devices may overload the channel and would make the Gateways exceed the duty cycle limitation, most devices use the Unconfirmed type of message (operators set the fee for downlink traffic much more expensive compared to uplink). So, unlike in unslotted ALOHA, devices are not aware of packet losses and do not retransmit them following a failed reception—they just operate according to their duty cycles to send data at the instants defined by the application. In such a setup, the crucial measure of LoRaWAN performance is Packet Delivery Ratio (*PDR*) and utilization $U = PDR \times v$, where v is the channel load.

Modeling LoRaWAN performance needs to take into account several aspects:

- transmissions using CSS are robust with respect to interference and can survive overlapping transmissions leading to the *capture effect* [4], [5], [6], [7], [8];
- successful packet delivery also depends on channel conditions (e.g., Rayleigh fading [9], [10]) that may greatly influence the packet reception for transmissions over long distances (e.g., several kilometers in case of LoRa networks);
- improving *PDR* when devices cannot rely on ACKs for retransmissions of lost packets requires some transmission redundancy in the form of inter-frame Error Correction Codes (ECC) or transmission repetitions [11], [10].

Most of the existing reception models for LoRaWAN disregard the arrival timing of an interfering frame with respect to the frame of interest [12], [13]. Unlike these models, we propose a model that distinguishes, on the one hand, the interference created by earlier transmissions with respect to the frame of interest, and on the other hand, the interference by the frames arriving later on. The former may both hinder receiver locking and then jam the reception, whereas the latter only jams the reception. For instance, the SX1301 chip does not seek to receive a new preamble for the same SF and frequency channel it is already busy with. So the model derived

below matches the behavior of the gateways based on this chip, whereas it represents a worst case scenario for newer SX1302-based gateways.

The model is thus more conservative than the previous ones and its results lead us to make three observations. First, it puts back under the spotlight the often overlooked fact that repeating frames is (almost) always beneficial, even though the natural reaction to the idea of repetition is that the extra packet transmissions merely create more collisions, which they do. However, the overall effect is an improved Packet Delivery Ratio (*PDR*). Second, as soon as the node density becomes notable and collisions have a similar impact on losses as attenuation, adding the weaker *SF6* modulation into the cell list of transmission parameters allows increasing the coverage range. Third, the model shows that the cell capacity sometimes grows with the distance to the gateway or with decreased node transmission power, a trend seldom observed in wireless networks.

II. Modeling *PDR* in LoRaWAN

In this section, we present the model for *PDR* in a LoRaWAN cell.

A. Assumptions

We assume that all devices using the same spreading factor *SF* (transmission duration of τ_j and data rate DR*j*) are at the same distance[1], and they contend for the same channel. In practice, devices adjust the value of *SF* using the ADR mechanism based on the experienced channel conditions in successful transmissions, so that the devices using the same *SF* effectively face similar average channel gains. Although devices may wake up at constant intervals, the superposition of traffics from a large number of devices using DR*j* forms a homogeneous Poisson process with intensity λ_j. We denote by $v_j = \lambda_j \tau_j$ the offered traffic in Erlang.

We consider that transmissions using different spreading factors are quasi-orthogonal so that inter-SF interference is negligible [15], [16], [17]. We also assume that the wireless channel is subject to Rayleigh fading [9], [10], [18]. Table I summarizes the notation.

B. Traditional ALOHA Model for LoRaWAN

In LoRaWAN, the probability H of receiving a frame when it is not subject to a collision is the following:

$$H = e^{-g_j} \tag{1}$$

as the fast fading gain follows an unit-mean exponential distribution. The threshold gain g_j is the value for which the reception power exceeds q_j:

$$g_j = \frac{\mathcal{N} q_j}{P_{\mathrm{t}}\, g(d)}. \tag{2}$$

[1]Outside of the first SF zone, there is little contrast between the channel gains for the nodes using the same SF. Collision capture unfairness is limited and can be modeled [14]

TABLE I
Notation

Frame duration at data rate DR*j* and *SFj*	τ_j
Aggregate packet generation intensity at DR*j*	λ_j
Offered traffic (in Erlang) at DR*j* and *SFj*	$v_j = \lambda_j\, \tau_j$
Channel utilization $PDR \times v_j =$	U
Average channel gain at distance d	$g(d)$
SNR threshold for DR*j* and *SFj*	q_j
SNR threshold for receiver locking at *SFj*	αq_j
Power gap for successful capture (typically 0 dB)	ξ
Transmission power	P_{t}
In-band noise power	$\mathcal{N}$
Probability of dominating thermal noise	H
PDR of unslotted ALOHA	$\boldsymbol{P}_{\mathrm{A}}$
PDR in LoRaWAN, capture model [8]	$\boldsymbol{P}_{\Sigma}$
PDR in LoRaWAN, our model	$\boldsymbol{P}_{\mathrm{S}}$
Number of repetitions of the application data	R

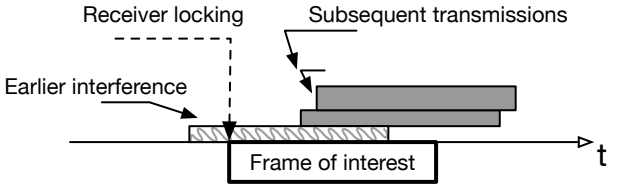

Fig. 1. Analyzed case of frame reception: successful reception of the Frame of interest depends on previous transmissions (considered as Earlier interference) and Subsequent transmissions.

Thus, the *PDR* of unslotted ALOHA is as follows:

$$\boldsymbol{P}_{\mathrm{A}} = H e^{-2v_j} \tag{3}$$

because a frame may also be lost whenever it intersects another earlier or later frame. This model is simple but we know that it is overly pessimistic: in reality, if the interference is weaker enough compared to the signal of interest, then it does not disrupt reception. The interference may even go totally unnoticed in some cases, a situation which the model below incorporates.

C. Modeling Successful Reception in LoRaWAN

Figure 1 presents the analyzed case of what happens when a given transmission represented as the Frame of interest collides with other transmissions in LoRaWAN. To receive the Frame of interest successfully, the Gateway needs to lock on the signal and then, correctly decode the frame. For the gateways based on the SX1301 chips, a reception at a given *SF* on a given channel forbids locking on a frame transmitted with the same *SF* and on the same frequency band as long as reception lasts (it is no longer the case for the current SX1302 chips). Previous transmissions (represented as Earlier interference in the figure) may compromise receiver locking and then they can add up to the interference from Subsequent transmissions arriving after the start of the Frame of interest. Note that a later colliding frame in Subsequent transmissions may arrive after the transmission of a frame in Previous transmissions.

To shed light on the relationship between traffic load and the probability of successful packet delivery at a given distance, we first analyze the probability of transmission success in the case of thermal noise and the presence of N newly arriving

interfering packets on top of constant earlier interference. Then, Section II-E considers a refined locking condition under which reception starts even though there is a transmission of a previous frame on the channel: if the reception power of the earlier frames is well below the receiver sensitivity, the receiver is not able to detect it, and thus, it is free to lock on the new incoming frame. When the load increases with a large number of contending devices, more and more frames find the channel busy upon arrival, so collisions and capture are more and more frequent and the model in Section II-E will reflect this aspect as precisely as possible.

In the analysis below, we do not consider that the likelihood of overcoming thermal noise and interference is independent as it was assumed in previous work [12], [19], [20], [21], [22], [16], [14] or that only collisions matter [23].

D. PDR when Facing N Subsequent Transmissions

Consider a Frame of interest transmitted against N other overlapping transmissions, on top of a baseline constant interference and noise. Two conditions need to be satisfied for successful packet delivery:

1) the fast fading channel gain for this transmission is above g_j, so that the received power is above the sensitivity for a given *SF*,
2) and the Frame of interest dominates the interference power by factor ξ.

The Gateway can correctly receive a frame subject to collisions, as long as its power margin is sufficient for successful demodulation. We distinguish between the interference that pre-exists on the channel (Earlier interference) when the Frame of interest arrives and the sum of the transmission power of subsequent frames. For the sake of convenience, we express the pre-existing interference power as a fraction α of the successful reception power: $\alpha\, q_j\, \mathcal{N}$.

In the derivation, we use the density of the sum of N variables following the $\exp(1)$ distribution: $f_\Sigma(N,x) = \frac{e^{-x}\, x^{N-1}}{(N-1)!}$. In presence of the earlier interference, the distribution of the sum of the fast fading gains with N additional colliding frames is shifted to the right: $f_\Sigma(N, x-\alpha g_j)$.

The probability of successful reception of a Frame of interest transmitted against N other overlapping transmissions is the probability $\boldsymbol{p}_{\rm i}$ that the Frame of interest dominates both the thermal noise and the interference (see derivation in Appendix A):

$$\begin{aligned}\boldsymbol{p}_{\rm i}(N,\alpha) &= \int_{\alpha g_j}^{\infty} f_\Sigma(N, x-\alpha g_j) \int_{\max(g_j,\xi x)}^{\infty} e^{-y}\, dy\, dx \\ &= \frac{1}{(N-1)!}\left[e^{-g_j}\gamma\left(N, (\frac{1}{\xi}-\alpha)g_j\right)\right. \\ &\left. + \frac{e^{-\xi\alpha g_j}}{(\xi+1)^N}\,\Gamma\left(N, (\xi+1)(\frac{1}{\xi}-\alpha)g_j\right)\right],\end{aligned} \tag{4}$$

where $\gamma(N,x)$ is the lower incomplete gamma function and $\Gamma(N,x)$ is the upper incomplete gamma function.

E. Condition for Receiver Locking

If we consider that the Gateway cannot lock on reception below the received power of αq_j for *SFj*, then we can refine the usual "ALOHA with capture" condition, which requires an empty channel when frame reception starts.

The frame reception *SNR* (Signal to Noise Ratio) is below αq_j when the fast fading channel gain is below αg_j, so the probability that the received power of $N \geq 1$ earlier frames is below αg_j is the following:

$$\boldsymbol{p}_{\rm L}(N) = \int_0^{\alpha g_j} f_\Sigma(N,x)\, dx = \frac{\gamma(N, \alpha g_j)}{(N-1)!}. \tag{5}$$

For one or more earlier frames, the overall receiver locking probability $\boldsymbol{P}_{\rm L}$ is the probability that the sum of the channel gains of transmissions occupying the channel when the Frame of interest starts be below αg_j:

$$\boldsymbol{P}_{\rm L}(v_j) = \sum_{N=0}^{\infty} \frac{(v_j)^N}{N!\, e^{v_j}} \boldsymbol{p}_{\rm L}(N+1). \tag{6}$$

F. PDR Considering Earlier Interference

Once the Gateway locks on the reception, it is still possible to lose the frame if later ones interfere with it. We make a conservative approximation: *"whenever reception starts in presence of at least one frame, the interference is at the level of $\alpha q_j \mathcal{N}$ and it remains for the rest of the frame reception"*. In Figure 1, all interfering signals add up to each other, but a later colliding frame could arrive after the earlier one has completed. In reality, there is a good chance that the earlier frame leaves the channel before its signal adds up to all other frames.

We denote by $\boldsymbol{P}_0$ the probability to receive a frame if it finds an empty channel (so that 0 or more frames interfere with it during its transmission):

$$\boldsymbol{P}_0(v_j) = e^{-g_j - v_j} + \sum_{N=1}^{\infty} \frac{(v_j)^N}{N!\, e^{v_j}} \boldsymbol{p}_{\rm i}(N,0), \tag{7}$$

whereas $\boldsymbol{P}_{1^+}$ is the probability of receiving a frame if at least one transmission had started in a window of duration τ_j before the start of the transmission:

$$\boldsymbol{P}_{1^+}(v_j) = \boldsymbol{P}_{\rm L}(v_j)\, \boldsymbol{P}_{\rm i}(v_j), \tag{8}$$

where $\boldsymbol{P}_{\rm i}$ is the probability of overcoming the interference with a pre-existing interference level of $\alpha\, q_j\, \mathcal{N}$ conditioned by the receiver locked on the frame, which happens with probability $\boldsymbol{P}_{\rm L}$. We obtain the expression for $\boldsymbol{P}_{\rm i}$ in a similar way to Eq. 7:

$$\boldsymbol{P}_{\rm i}(v_j) = e^{-g_j - v_j} + \sum_{N=1}^{\infty} \frac{(v_j)^N}{N!\, e^{v_j}} \boldsymbol{p}_{\rm i}(N,\alpha); \tag{9}$$

since the interference is below αg_j and we consider the case in which $\alpha < 1$ with no subsequent transmissions, so meeting the minimum channel gain of g_j is sufficient to dominate earlier interference and the first term of $\boldsymbol{P}_{\rm i}$ is similar to the first term of Eq. 7. The summation of the second term corresponds to the cases in which subsequent frames join the earlier interference.

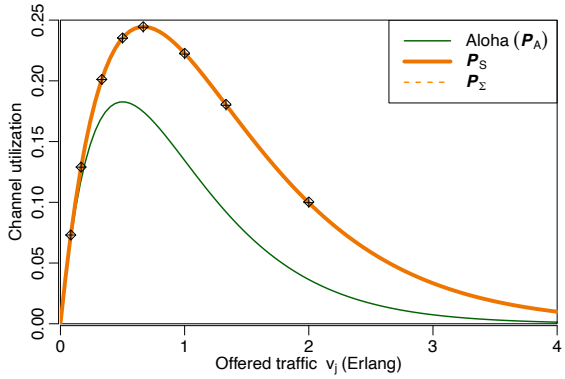

Fig. 2. Channel utilization as a function of load for three *PDR* models compared with simulation results (crosses and rhombi). Reception is subject to no or low earlier interference and dominating the sum of interference by factor $\xi = 0$ dB, distance of 2.5 km. Earlier interference is never below the locking threshold, so $\boldsymbol{P}_\Sigma$ [8] and $\boldsymbol{P}_S$ perfectly overlap.

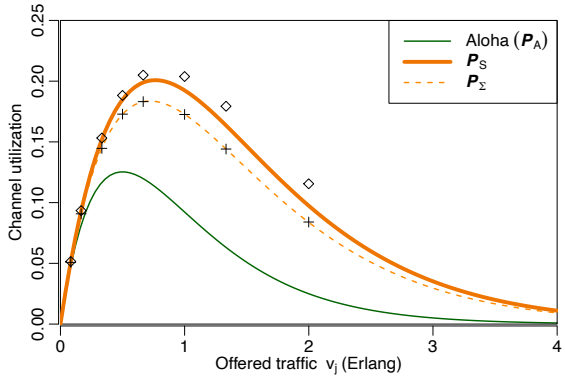

Fig. 3. Channel utilization as a function of load for three *PDR* models compared with simulation results (crosses and rhombi). Reception is subject to no or low earlier interference and dominating the sum of interference by factor $\xi = 0$ dB, distance of 7.5 km. Compared to the simulation results, at high load and at this distance, the earlier interference approximation causes the model to slightly underestimate *PDR* (the difference between rhombi and the $\boldsymbol{P}_S$ curve).

Finally, for all scenarios of earlier interference and subsequent transmissions, we obtain the *PDR* of our model, with the above approximation, denoted $\boldsymbol{P}_S$:

$$\boldsymbol{P}_S(v_j) = e^{-v_j}\,\boldsymbol{P}_0(v_j) + (1 - e^{-v_j})\,\boldsymbol{P}_{1^+}(v_j). \qquad (10)$$

This model extends the model $\boldsymbol{P}_\Sigma(v_j) = e^{-v_j}\,\boldsymbol{P}_0(v_j)$ in which packet reception is conditioned on the empty channel when a frame arrives [8].

G. Numerical Examples

Figures 2 and 3 show the channel utilization defined as $U = PDR \times v_j$ (where *PDR* corresponds to unslotted ALOHA $\boldsymbol{P}_A$, empty channel upon arrival $\boldsymbol{P}_\Sigma$, and our model $\boldsymbol{P}_S$) vs. load v_j for devices located relatively close (2.5 km) and far away (7.5 km) from the Gateway. We assume *SF12*, the Gateway antenna 15 m above the ground with 6 dB antenna gain, and the Okumura-Hata suburban channel attenuation model. Earlier interference is never below the locking threshold when devices are close as all receptions are well above sensitivity (see Figure 2), whereas a significant number of frames are captured even in presence of earlier interference when devices are located farther away (see Figure 3).

In these figures, we compare the analytical results of the models with the output of a dedicated Python discrete-event simulator, which can simulate losses either whenever two frames overlap or based on interference level and timing. The model and simulation perfectly agree for $\boldsymbol{P}_\Sigma$ at all distances (confidence intervals are not shown, they are in the order of 1 percentage point). For high loads and for devices located farther away, the approximation used to compute $\boldsymbol{P}_S$ results in a slightly underestimated probability of successful reception as the pre-existing frames sometimes do not add up to all the later ones (see Figure 3).

III. LoRaWAN Utilization and Cell Capacity for Packet Repetition and Receiver Diversity

As for all spread-spectrum transmission technologies, there is a tradeoff between capacity and range in LoRaWAN—they both depend on the level of *PDR* for which they are defined: for instance, the range and/or capacity for 95% *PDR* are much smaller than for 60%. For a given *PDR*, when the distance increases, lost packets due to attenuation and fading reduce the acceptable collision rate.

To illustrate this tradeoff, we focus on two cases: *PDR* of 95% and 60%. For many IoT applications, 95% *PDR* is sufficient and 60% *PDR* at the LoRaWAN packet layer can be acceptable if redundancy is used to improve application data delivery probability (e.g., up to 84% for simple packet repetition).

When an inter-frame Error Correction Code (ECC) mechanism is used, for instance with coding rate $CR = 0.5$ (two packets sent for one packet of data), the network needs to maintain *PDR* above the *CR* with a margin (e.g., 60% for $CR = 0.5$). In this case, the offered traffic at which the *PDR* drops below 60% needs to be at least twice the load at which *PDR* is 95%. Otherwise, an ECC mechanism would actually make things worse because the traffic increase corresponding to redundancy is not compensated by the benefit of error correction.

We can also improve the probability of successfully receiving application data with receiver diversity (the deployment of multiple Gateways). We investigate both redundancy and diversity in this section.

A. Systematic Repetition

Systematic frame repetition is a double-edge sword: it improves the probability of application data delivery at the cost of an increase in the effective load generated in the network, which increases collisions and thus packet losses. As we consider Unconfirmed LoRaWAN data frames, repetition of a frame may incur superfluous transmissions and collisions even if the first transmission was successfully received.

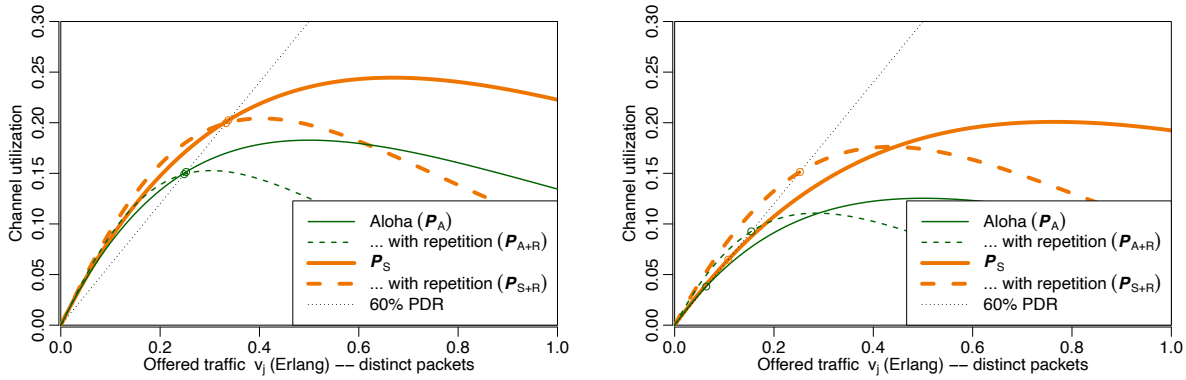

(a) Distance 2.5 km

(b) Distance 7.5 km

Fig. 4. Utilization with and without systematic repetition. The straight dotted line corresponds to *PDR* of 60%.

For unslotted ALOHA, the probability of successful packet delivery with R repetitions ($R = 2$ for simple repetition) is the following:

$$\boldsymbol{P}_{\text{A+R}}(v_j) = 1 - (1 - H\, e^{-2Rv_j})^R, \tag{11}$$

as each packet has R reception opportunities and the effective offered load becomes $R\, v_j$. Similarly,

$$\boldsymbol{P}_{\text{S+R}}(v_j) = 1 - (1 - \boldsymbol{P}_{\text{S}}(R\, v_j))^R. \tag{12}$$

Figure 4 shows the utilization based on $\boldsymbol{P}_{\text{A}}$, $\boldsymbol{P}_{\text{A+R}}$, and $\boldsymbol{P}_{\text{S}}$, $\boldsymbol{P}_{\text{S+R}}$. The maximum capacity for 60% *PDR* is determined by the point at which the curves intersect the black dotted line—they almost coincide for $\boldsymbol{P}_{\text{A}}$ and $\boldsymbol{P}_{\text{A+R}}$ as well as for $\boldsymbol{P}_{\text{S}}$ and $\boldsymbol{P}_{\text{S+R}}$. Still, repetition gives a little bit more headroom: the curves with repetition are noticeably above the curves with no repetition to the left of the 60% *PDR* crosspoint.

At a short distance (see Figure 4(a)), the results of our model are similar to that for ALOHA but allow for a higher utilization. Note that repetition is not beneficial for *PDR* lower than 60% both for ALOHA and our model (the dashed curves are below the solid ones to the right of the intersection point with the black dotted line).

Farther away (see Figure 4(b)), repeating each frame allows maintaining the desired *PDR* up to a much higher load meaning that capacity is increased: the curve with repetition crosses the black dotted line further to the right, more than doubling the acceptable load of distinct packets (i.e., half of effective packet transmissions). Repetition gives us an important gain of capacity: the load at which *PDR* drops below 60% increases from 0.064 to 0.154 for ALOHA (increase by 141%) and from 0.108 to 0.253 (increase by 134%) for our model!

IV. Increasing the Coverage Range with *SF6*

The *SF* boundaries in a cell form a set of annuli around the Gateway in which devices share the same value of *SF* because a device needs to configure its *SF* to obtain a desired level of *PDR* for a given distance to the Gateway. In a LoRWAN cell, *SF* allocation needs to strike a balance between losses due to attenuation and to collisions, knowing that switching to a higher *SF* has a strong influence on both aspects, in opposite directions. Interestingly, in a relatively dense cell, for instance with 90 nodes per km^2, it is more effective to add *SF6* to the list of useable *SFs* (*SF6* is a known LoRa transmission parameter, but it is not part of the LoRaWAN standard) than using an hypothetical *SF13*.

Figure 5 illustrates this case. To allocate the *SFs*, we find by dichotomy the range at which the *PDR* drops below a given threshold (60% in the figures) for the first *SF*, and then, we switch to the next *SF* etc. Both figures assume enabled repetitions and show $H_{\text{R}} = 1 - (1 - H)^2$. Although the coverage by *SF6* is limited, it significantly unloads the higher *SFs* to eventually increase cell capacity with 30% more nodes. Extrapolating the coverage from *SF10*, *SF11*, *SF12* to hypothetical *SF13* would allow to extend capacity by only about 100 more nodes.

V. Increased Load Capacity with More Nodes that are Further Away

As in Section III-A, we consider once again a set of nodes, all at the same distance from the Gateway. For the proposed model, it is remarkable that the load for which the *PDR* remains above a given value grows with the distance, even though more frames are lost due to attenuation if the traffic is light. The increase in cell capacity stems from the fact that, at a given distance, there are cases in which the receiver remains available for reception even though a transmission is ongoing because the channel gain is low enough so that the receiver ignores this weak transmission.

In Figure 6, the attainable load increase appears clearly, before the communication range limit become preeminent. Incidentally, in this figure, we can note that it is generally preferable to repeat a transmission at *SFX* than to transmit a packet once at higher *SF(X+1)*. This comparison is relevant because the duration of two transmissions at *SFX* is almost equal to the duration of one transmission at *SF(X+1)* so both choices drain similar energy, but the cell capacity is markedly different.

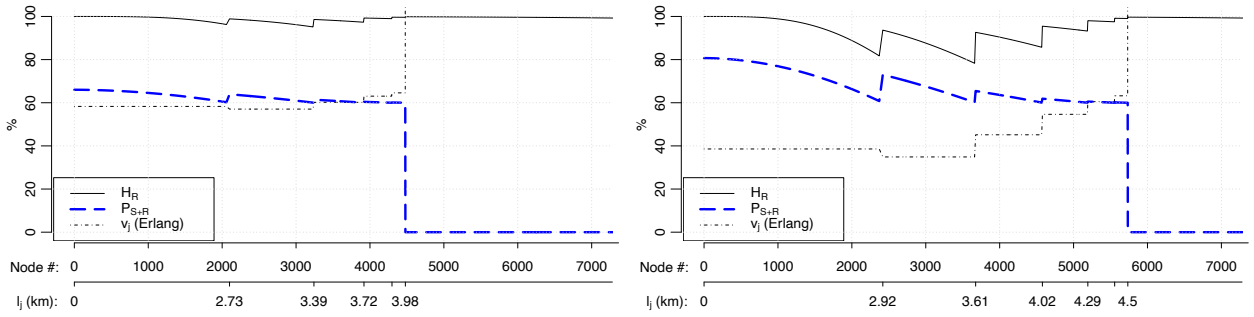

(a) *SF7* to *SF12* (b) *SF6* to *SF12*

Fig. 5. *SF* allocation vs. distance, without and with *SF6*, there is an infinite number of nodes in the unbounded *SF12* zone and *PDR* tends to 0. l_j denotes the distance of the farthest node using DR*j*. Spatial density of 90 nodes per km^2.

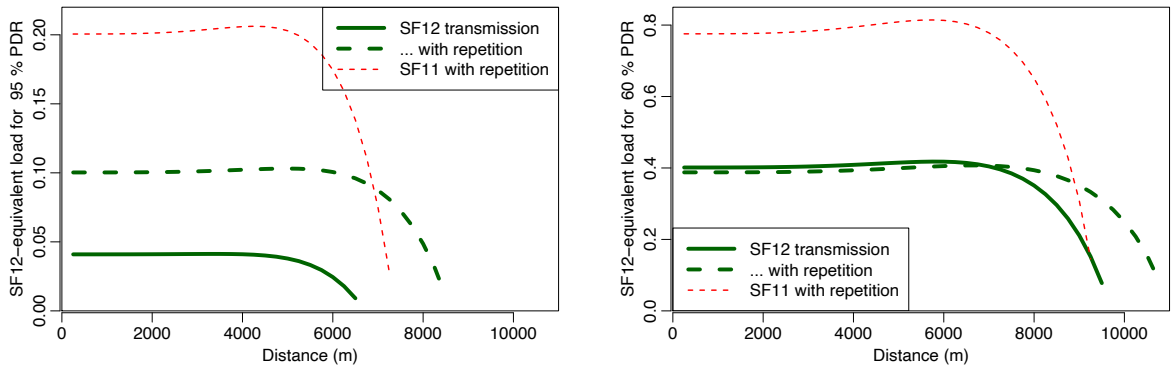

(a) 95% *PDR* (b) 60% *PDR*

Fig. 6. Load limit for the indicated *PDR* as a function of the distance.

VI. Conclusion

Taking into account the frame arrival timing for modeling *PDR* in LoRaWAN brings several surprising results. In particular, we can observe a capacity improvement even though more packets are lost due to channel attenuation. The proposed model also confirms that transmissions need to be redundant (by means of using inter-packet ECC or at least with simple repetitions), as otherwise, data reception is either unreliable or we need to have both light traffic and good channel gain. Our model represents the operation of the Semtech SX1301 chip, but SX1302, its successor does not have the same limitation: receiver locking remains possible for the same SF and the frequency channel as an ongoing reception. So, this possibility has the potential to improve capacity considerably [8].

Acknowledgments

This work has been partially supported by the French Ministry of Research projects PERSYVAL-Lab under contract ANR-11-LABX-0025-01 and DiNS under contract ANR-19-CE25-0009-01.

Appendix A
Probability of successful reception of a Frame of interest

The probability of successful reception of a Frame of interest transmitted in presence of N other overlapping transmissions is the probability $\boldsymbol{p}_{\mathrm{i}}$ that the Frame of interest dominates both the thermal noise and the interference:

$$\begin{aligned}
\boldsymbol{p}_{\mathrm{i}}(N,\alpha) &= \int_{\alpha g_j}^{\infty} f_{\Sigma}(N, x-\alpha g_j) \int_{\max(g_j,\xi x)}^{\infty} e^{-y}\, dy\, dx \\
&= \int_{0}^{\infty} f_{\Sigma}(N, x') \int_{\max(g_j,\xi(x'+\alpha g_j))}^{\infty} e^{-y}\, dy\, dx' \\
&= \int_{0}^{g_j(\frac{1}{\xi}-\alpha)} f_{\Sigma}(N, x') \int_{g_j}^{\infty} e^{-y}\, dy\, dx' \\
&\quad + \int_{g_j(\frac{1}{\xi}-\alpha)}^{\infty} f_{\Sigma}(N, x') \int_{\xi(x'+\alpha g_j)}^{\infty} e^{-y}\, dy\, dx' \\
&= \frac{e^{-g_j}}{(N-1)!} \int_{0}^{g_j(\frac{1}{\xi}-\alpha)} e^{-x'} {x'}^{N-1}\, dx' \\
&\quad + \int_{g_j(\frac{1}{\xi}-\alpha)}^{\infty} \frac{e^{-x'} {x'}^{N-1}}{(N-1)!} e^{-\xi(x'+\alpha g_j)}\, dx'
\end{aligned}$$

$$= \frac{1}{(N-1)!}\left[e^{-g_j}\gamma\left(N, g_j(\frac{1}{\xi}-\alpha)\right) + e^{\xi\alpha g_j}\int_{g_j(\frac{1}{\xi}-\alpha)}^{\infty}\frac{[(\xi+1)x']^{N-1}}{(\xi+1)^{N-1}}e^{-(\xi+1)x'}dx'\right]$$

Setting $u = (\xi+1)x'$, we obtain:

$$\boldsymbol{p}_{\mathrm{i}}(N,\alpha) = \frac{1}{(N-1)!}\left[e^{-g_j}\gamma\left(N, g_j(\frac{1}{\xi}-\alpha)\right) + \frac{e^{\xi\alpha g_j}}{(\xi+1)^N}\int_{(\xi+1)(\frac{1}{\xi}-\alpha)g_j}^{\infty}u^{N-1}e^{-u}\,du\right]$$

And finally:

$$\boldsymbol{p}_{\mathrm{i}}(N,\alpha) = \frac{1}{(N-1)!}\left[e^{-g_j}\gamma\left(N, (\frac{1}{\xi}-\alpha)g_j\right) + \frac{e^{-\xi\alpha g_j}}{(\xi+1)^N}\Gamma\left(N, (\xi+1)(\frac{1}{\xi}-\alpha)g_j\right)\right] \tag{13}$$

where $\gamma(N,x)$ is the lower incomplete gamma function and $\Gamma(N,x)$ is the upper incomplete gamma function.

REFERENCES

[1] LoRa™ Alliance, "A Technical Overview of LoRa and LoRaWAN," 2015.

[2] N. Sornin *et al.*, "LoRaWAN Specification v1.1," 2017. [Online]. Available: https://lora-alliance.org/resource-hub/lorawantm-specification-v11

[3] N. Abramson, "THE ALOHA SYSTEM: Another Alternative for Computer Communications," in *Proceedings of the Fall Joint Computer Conference*, New York, NY, USA, 1970, pp. 281–285.

[4] L. G. Roberts, "ALOHA Packet System with and without Slots and Capture," *SIGCOMM Comput. Commun. Rev.*, vol. 5, no. 2, p. 28–42, Apr. 1975.

[5] C. Lau and C. Leung, "Capture Models for Mobile Packet Radio Networks," *IEEE Trans. Commun.*, vol. 40, pp. 917–925, 1992.

[6] A. Kochut, A. Vasan, A. U. Shankar, and A. K. Agrawala, "Sniffing Out the Correct Physical Layer Capture Model in 802.11b," in *IEEE ICNP*, Berlin, Germany, 2004, pp. 252–261.

[7] K. Whitehouse, A. Woo, F. Jiang, J. Polastre, and D. Culler, "Exploiting the Capture Effect for Collision Detection and Recovery," in *Proc. the 2nd IEEE Workshop on Embedded Networked Sensors*, 2005, p. 45–52.

[8] T. Attia, M. Heusse, and A. Duda, "Message in Message for Improved LoRaWAN Capacity," in *IEEE International Conference on Computer Communications and Networks (ICCCN)*, Jul. 2021.

[9] T. Attia, M. Heusse, B. Tourancheau, and A. Duda, "Experimental Characterization of LoRaWAN Link Quality," in *Proc. IEEE GLOBECOM*, 2019, pp. 1–6.

[10] U. Coutaud, M. Heusse, and B. Tourancheau, "High Reliability in LoRaWAN," in *Proceedings of IEEE PIMRC*, London (virtual conference), United Kingdom, Aug. 2020.

[11] Y. Birk and Y. Keren, "Judicious Use of Redundant Transmissions in Multichannel ALOHA Networks with Deadlines," *IEEE Journal on Selected Areas in Communications*, vol. 17, no. 2, pp. 257–269, 1999.

[12] O. Georgiou and U. Raza, "Low Power Wide Area Network Analysis: Can LoRa Scale?" *IEEE Wireless Communications Letters*, vol. 6, no. 2, Apr. 2017.

[13] A. Hoeller, R. D. Souza, O. L. Alcaraz López, H. Alves, M. de Noronha Neto, and G. Brante, "Analysis and Performance Optimization of LoRa Networks With Time and Antenna Diversity," *IEEE Access*, vol. 6, 2018.

[14] J. M. d. S. Sant'Ana, A. Hoeller, R. D. Souza, S. Montejo-Sánchez, H. Alves, and M. d. Noronha-Neto, "Hybrid coded replication in LoRa networks," *IEEE Transactions on Industrial Informatics*, vol. 16, no. 8, pp. 5577–5585, 2020.

[15] C. Goursaud and J.-M. Gorce, "Dedicated Networks for IoT: PHY/MAC State of the Art and Challenges," *EAI Endorsed Transactions on Internet of Things*, vol. 1, no. 1, 10 2015.

[16] A. Mahmood, E. Sisinni, L. Guntupalli, R. Rondon, S. A. Hassan, and M. Gidlund, "Scalability analysis of a lora network under imperfect orthogonality," *IEEE Transactions on Industrial Informatics*, 2018.

[17] M. Heusse, T. Attia, C. Caillouet, F. Rousseau, and A. Duda, "Capacity of a LoRaWAN Cell," in *Proc. ACM MSWiM '20*, 2020, pp. 131–140.

[18] X. Le, B. Vrigneau, M. Gautier, M. Mabon, and O. Berder, "Energy/Reliability Trade-off of LoRa Communications over Fading Channels," in *IEEE ICT 2018, Saint Malo, France, June 26-28, 2018*, pp. 544–548.

[19] Z. Li, S. Zozor, J.-M. Brossier, N. Varsier, and Q. Lampin, "2D Time-Frequency Interference Modelling Using Stochastic Geometry for Performance Evaluation in Low-Power Wide-Area Networks," in *2017 IEEE ICC*, May 2017.

[20] A. Waret, M. Kaneko, A. Guitton, and N. El Rachkidy, "LoRa Throughput Analysis with Imperfect Spreading Factor Orthogonality," *IEEE Wireless Communications Letters*, 2018.

[21] J. Petäjäjärvi, K. Mikhaylov, M. Pettissalo, J. Janhunen, and J. Iinatti, "Performance of a low-power wide-area network based on LoRa technology: Doppler robustness, scalability, and coverage," *International Journal of Distributed Sensor Networks*, vol. 13, no. 3, 2017.

[22] K. Mikhaylov, J. Petäjäjärvi, and T. Hänninen, "Analysis of Capacity and Scalability of the LoRa Low Power Wide Area Network Technology," in *22th European Wireless Conference*, May 2016.

[23] Q. Song, X. Lagrange, and L. Nuaymi, "Evaluation of Macro Diversity Gain in Long Range ALOHA Networks," *IEEE Comm. Letters*, vol. 21, no. 11, pp. 2472–2475, 2017.